Forschungszentrum Karlsruhe

Technik und Umwelt

Wissenschaftliche Berichte

FZKA 6560

Magnetohydrodynamic flow in the liquid phase for the EVOLVE boiling scenario

L. Bühler

Institut für Kern- und Energietechnik
Programm Kernfusion

Forschungszentrum Karlsruhe GmbH, Karlsruhe
2001

Magnetohydrodynamic flow in the liquid phase for the EVOLVE boiling scenario

Abstract

In the EVOLVE concept for a fusion blanket a boiling scenario is proposed where a number of permanent vertical vapor channels are formed in a horizontal layer of liquid lithium. The present analysis focuses on the flow of the electrically conducting liquid phase in the presence of a strong uniform horizontal magnetic field. The cross section of vapor channels is circular if surface tension dominates magnetic forces. In the other case a stretching of the liquid-vapor interface along magnetic field lines is observed and contours become possible where a major part of the interface is straight and aligned with the field. For strong magnetic fields the liquid flow exhibits several distinct subregions. Most of the liquid domain is occupied by inviscid cores. These are separated from each other by parallel layers that spread along the field lines which are tangential to the vapor channel. In the core between two parallel layers the flow direction is preferentially oriented along magnetic field lines, while outside these layers the flow is perpendicular to the field. The magnetohydrodynamic pressure drop in the liquid phase is relatively small.

Magnetohydrodynamische Strömungen in der flüssigen Phase für das EVOLVE Siedeszenario

Zusammenfassung

Im EVOLVE Konzept eines Fusionsblankets wird ein Siedeszenario vorgeschlagen, bei dem sich permanente vertikale Dampfkanäle in einer horizontalen Flüssigkeitsschicht bilden. Gegenstand der Untersuchung ist die Strömung in der elektrisch leitenden flüssigen Phase unter der Einwirkung eines homogenen horizontalen Magnetfeldes. Wenn die Oberflächenkräfte stärker sind als die magnetischen Kräfte, besitzen die Dampfkanäle einen nahezu kreisförmigen Querschnitt. Im anderen Fall beobachtet man eine Streckung der Querschnitte entlang magnetischer Feldlinien. Diese Streckung kann dazu führen, dass große Teile der Kontur gerade werden und sich entlang der Feldlinien ausrichten. Für starke Magnetfelder entstehen mehrere charakteristische Strömungsbereiche. Dabei spielen die reibungsfreien Kernströmungsgebiete eine entscheidende Rolle. Entlang den zur Kontur tangentialen Feldlinien entstehen viskose parallel Scherschichten, die jeweils zwei Kernströmungsgebiete voneinander trennen. Zwischen zwei parallelen Schichten strömt das Fluid vorwiegend entlag magnetischer Feldlinien, während außerhalb der Schichten die Strömung senkrecht zum Magnetfeld verläuft. Der magnetohydrodynamische Druckverlust in der flüssigen Phase ist relativ klein.

Magnetohydrodynamic flow in the liquid phase for the EVOLVE boiling scenario

Contents

1 Introduction **1**

2 Formulation **2**

3 Numerical solution **5**

4 Asymptotic analysis **9**
- 4.1 The Hartmann layers 9
- 4.2 The core 11
- 4.3 The interface 12
- 4.4 Flow pattern 14
- 4.5 Three-dimensional considerations 17

5 Conclusions **20**

1 Introduction

Efficient heat removal at high temperatures is a key issue for blankets in nuclear fusion applications. The EVOLVE (Evaporation of Lithium and Vapor Extraction) concept is a recently proposed candidate for such a blanket (Anderson, Murphy, Sawan, Sviatoslavsky, Corradini and Malang (2000)) due to the large heat of evaporation of lithium. The latter reference supports a potential boiling scenario where permanent vertical vapor channels in horizontal layers of liquid lithium are held open by a balance between vapor momentum, friction and magnetic field effects. The layers of liquid are located on horizontal trays. One vapor channel is schematically shown in Fig. 1.

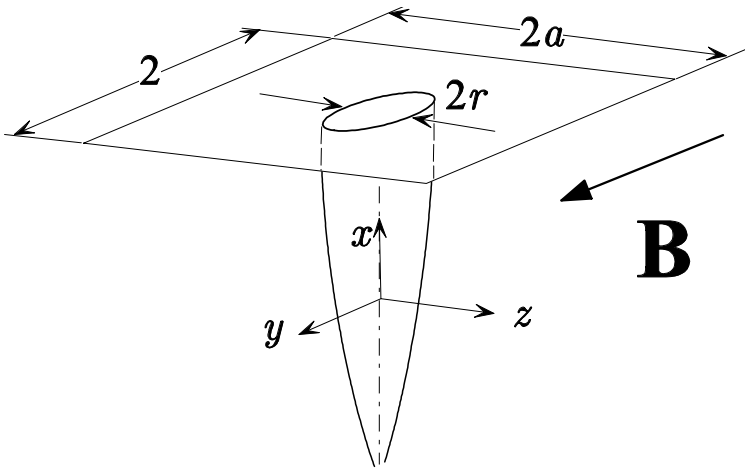

Figure 1: Geometry of a vapor channel located in a periodic arrangement.

In the following we will not analyze the heat transfer details. We assume that such a boiling scenario exists and we analyze the two-dimensional magnetohydrodynamic flow in the liquid phase in a plane perpendicular to these vapor channels. We give estimates for the pressure drop required to drive the liquid to the interface. We show further that the shape of vapor channels' cross section may deviate from a circular cross section that would be expected in the absence of a magnetic field. In case of a horizontal magnetic field the channels are elongated along field lines.

It is not clear that a boiling scenario as proposed for EVOLVE exists really. This scenario is based on the two assumptions, that strong magnetic fields suppress turbulent movements of the liquid metal, and that it is possible to trigger the nucleation sites required for the formation of vapor channels at the strongly heated bottom plate. Stable vapor jets or columns seem possible in non-magnetic boiling if the vapor velocity is below a certain threshold (see e.g. Whalley (1987) p.137-139). The start-up of such a flow pattern and the stability of vapor channels in strong magnetic fields remain to be seen.

2 Formulation

In the following analysis we assume a steady state flow of a fluid with density ρ, kinematic viscosity ν and electric conductivity σ for which inertia forces are negligible in comparison with electromagnetic forces. The governing equations then reduce to

$$\nabla p = \frac{1}{Ha^2}\nabla^2 \mathbf{v} + \mathbf{j} \times \hat{\mathbf{y}}, \tag{1}$$

$$\mathbf{j} = -\nabla\phi + \mathbf{v} \times \hat{\mathbf{y}}. \tag{2}$$

We have a balance between pressure forces, viscous forces and Lorentz forces. The currents of density $\mathbf{j}$, given by Ohm's law, are driven by the gradient of a scalar electric potential and by the induced electric field due to the fluid motion. Conservation of mass and charge requires that

$$\nabla \cdot \mathbf{v} = 0, \quad \nabla \cdot \mathbf{j} = 0. \tag{3}$$

Here, the variables p, ϕ, $\mathbf{v}$, and $\mathbf{j}$ denote the pressure, the electric potential, the velocity vector and the electric current density scaled by the reference quantities $\sigma v_0 B^2 L$, $v_0 BL$, v_0 and $\sigma v_0 B$, respectively. The characteristic velocity v_0 is given by the rate of evaporation at the interface between vapor and liquid and L is a typical length scale of the problem in the plane of the vapor channel's cross section. For circular vapor channels L would be the radius. For periodically occurring vapor channels L is the half spacing between neighboring channels, measured along magnetic field lines. The horizontal magnetic field $\mathbf{B} = B\hat{\mathbf{y}}$ has a magnitude B and an orientation along the y-coordinate perpendicular to the vapor channel. For details of the geometry and coordinate systems see Fig. 2.

The square of the Hartmann number

$$Ha = LB\sqrt{\frac{\sigma}{\rho\nu}} \tag{4}$$

measures the ratio of electromagnetic forces to viscous forces. For applications in nuclear fusion Ha is typically on the order of 10^3 to 10^4. In the present case the size of the vapor channels L is not as large as the dimensions encountered in usual duct flows, but large enough that the Hartmann number is still very high, $Ha \gg 1$. The assumption that inertia is negligible compared to electromagnetic forces is justified for slow motions with typical velocity v_0 for which the interaction parameter

$$N = \frac{\sigma L B^2}{\rho v_0} \tag{5}$$

is large, $N \gg 1$.

We assume here for simplicity that variations of the vapor channel geometry along the channels' axes, along x in the present notation, are small. We consider a typical plane perpendicular to the channel's axis in which the derivatives of flow variables along x are small compared with the variations in this plane, i.e. $\partial_x \ll \partial_y, \partial_z$. The velocity has components in this plane only as $\mathbf{v} = v\hat{\mathbf{y}} + w\hat{\mathbf{z}}$ while the current density has a single

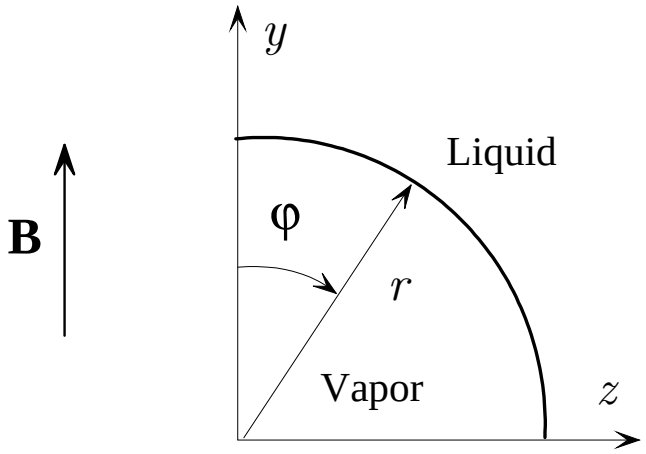

Figure 2: Sketch of geometry and coordinate system

component along the axis, $\mathbf{j} = j\hat{\mathbf{x}}$. We restrict the present analysis to cases which are symmetric with respect to the y-axis for which $w\,(z=0)=0$. The velocity component w is directly related by Ohm's law with the current density and by the momentum equation with the pressure gradient as $j = -\partial\phi/\partial x - w = \partial p/\partial z$. Since both, w and $\partial p/\partial z$ vanish due to symmetry along the y-axis the potential gradient along the axis of the vapor channel vanishes as well, $\partial\phi/\partial x = 0$. We assume that this holds also in some distance from the vapor channel, i.e. we do not consider here the regions near the bottom or the top of the liquid layer in which the currents close. This point is discussed again later in the report.

We satisfy the mass conservation equation identically by choosing a streamfunction formulation for the velocity field as

$$\mathbf{v} = \nabla \times (\psi\hat{\mathbf{x}}) = \partial_z\psi\hat{\mathbf{y}} - \partial_y\psi\hat{\mathbf{z}}. \tag{6}$$

Elimination of the pressure from (1) by taking the curl yields an equation for the x-component of vorticity $\boldsymbol{\omega} = \nabla\times\mathbf{v} = \omega\hat{\mathbf{x}}$ as

$$\nabla^2\omega + Ha^2\partial_y j = 0. \tag{7}$$

We eliminate the current by Ohm's law (2)

$$j = -w = \partial_y\psi \tag{8}$$

and find finally

$$\nabla^2\omega + Ha^2\partial_{yy}\psi = 0. \tag{9}$$

The definition of vorticity expressed in terms of the streamfunction leads to an equation that determines ψ as

$$\nabla^2\psi + \omega = 0. \tag{10}$$

The interface Γ between the vapor and the liquid is assumed to be free of tangential shear stress in the plane of the liquid motion.

$$\omega = 0 \quad \text{at } \Gamma. \tag{11}$$

We assume further that the mass flux transferred from the liquid to the vapor phase is uniform along the liquid-vapor interface This requires a uniform normal component of velocity

$$\mathbf{v} \cdot \mathbf{n} = -1 \quad \text{at } \Gamma, \tag{12}$$

with the unit normal $\mathbf{n}$ pointing from the vapor to the liquid. Expressed in terms of the streamfunction the above relation is equivalent to

$$\partial_t \psi = -1 \quad \text{at } \Gamma, \tag{13}$$

where t is a coordinate along the interface. Thus, the streamfunction ψ becomes proportional to the arc length measured along Γ.

3 Numerical solution

In order to get a first impression how the flow will arrange we assume that the geometry of the vapor channel remains circular and that the surrounding liquid domain is unbounded. Later we will relax the condition on the interface and allow for non-circular interface geometries which are determined by the solution of the problem. We introduce a polar coordinate system located in the center of the vapor channel. In these coordinates the Laplacean becomes

$$\nabla^2 = \left(\partial_{rr} + \frac{1}{r}\partial_r + \frac{1}{r^2}\partial_{\varphi\varphi} \right) \tag{14}$$

and the second derivative along y reads as

$$\partial_{yy} = \sin^2\varphi \left(\frac{1}{r^2}\partial_{\varphi\varphi} + \frac{1}{r}\partial_r \right) + \cos^2\varphi\, \partial_{rr} + 2\sin\varphi\cos\varphi \left(\frac{1}{r^2}\partial_\varphi - \frac{1}{r}\partial_{r\varphi} \right), \tag{15}$$

so that we can express the equations (9) and (10).

It is difficult to formulate a proper condition for the streamfunction as $r \to \infty$. A possible condition could be to assume a radial inflow especially for the case of weak magnetic fields,

$$\partial_r \psi = 0 \quad \text{as } r \to \infty. \tag{16}$$

However, as we will see below, for high Hartmann numbers the flow will be rather parallel to magnetic field lines than oriented along the radial direction. For strong magnetic fields, $Ha \gg 1$, a more appropriate condition could be to assume an inflow aligned with the magnetic field

$$\partial_y \psi = -\sin\varphi \frac{1}{r}\partial_\varphi \psi + \cos\varphi\, \partial_r \psi = 0 \quad \text{as } r \to \infty. \tag{17}$$

Both conditions (16) and (17) are equivalent as $r \to \infty$. At large distances from the interface the fluid velocity and its gradients become small so that

$$\omega \to 0 \quad \text{as } r \to \infty. \tag{18}$$

At the liquid vapor interface we have according to (13) and (11)

$$\psi = -\varphi\, r_\Gamma, \quad \omega = 0 \quad \text{at } r_\Gamma = 1. \tag{19}$$

For minimization of the computational effort we take profit of symmetries in the problem. There is no flow across the lines $\varphi = 0$ and $\varphi = \pi/2$ so that it is sufficient to concern only the sector between these lines with symmetry conditions

$$\begin{array}{lll} \psi = 0, & \omega = 0 & \text{at} \quad \varphi = 0, \\ \psi = -\frac{1}{2}\pi\, r_\Gamma, & \omega = 0 & \text{at} \quad \varphi = \frac{1}{2}\pi. \end{array} \tag{20}$$

For a numerical solution of (9) and (10) both would be desirable, to resolve the Hartmann layer at the liquid-vapor interface and to extend the computational domain to large values of $r_{\max}$. For that reason we apply a transformation to the radius such as

$$r = \exp(\xi). \tag{21}$$

This transformation gives a good resolution near $r = 1$ ($\xi = 0$) and, even if $r_{\max} \gg 1$, $\xi_{\max}$ has values of order unity. We multiply the equations by r^2 and find as an expression for the Laplacean

$$r^2\nabla^2 = \partial_{\xi\xi} + \partial_{\varphi\varphi} \tag{22}$$

and for

$$r^2\partial_{yy} = \sin^2\varphi\,\partial_{\varphi\varphi} + \cos^2\varphi\,\partial_{\xi\xi} + 2\sin\varphi\cos\varphi\,(\partial_\varphi - \partial_{\xi\varphi}) + \left(\sin^2\varphi - \cos^2\varphi\right)\partial_\xi. \tag{23}$$

The boundary condition (17) becomes independent of the position $\xi_{\max}$ where it is applied and reads now

$$r\partial_y\psi = -\sin\varphi\,\partial_\varphi\psi + \cos\varphi\,\partial_\xi\psi = 0 \quad \text{at } \xi = \xi_{\max}. \tag{24}$$

Computations using this condition at large radii ($\xi_{\max}$) show that the boundary condition is not perfect in order to describe the continuous spreading of the solution along z with increasing y. On the other hand, order of magnitude estimations reduce the governing equation $-\nabla^4\psi + Ha^2\partial_{yy}\psi = 0$ to

$$-\partial_\zeta^4\psi + \partial_{yy}\psi = 0, \tag{25}$$

where $\zeta = \sqrt{Ha}\,z$ is a stretched transverse coordinate. Such an equation allows for self-similar solutions as $\psi(\eta)$, where $\eta = \zeta/\sqrt{y}$. Now we may evaluate $\partial_y\psi = \partial_\eta\psi\,\partial_y\eta$ and $\partial_z\psi = \partial_\eta\psi\,\partial_z\eta$ and eliminate from both equations $\partial_\eta\psi$. This leads to a condition

$$2y\partial_y\psi + z\partial_z\psi = 0, \tag{26}$$

or when expressed in terms of the polar coordinates introduced above we find

$$-\sin\varphi\cos\varphi\,\partial_\varphi\psi + \left(\cos^2\varphi + 1\right)\partial_\xi\psi = 0 \quad \text{at } \xi = \xi_{\max}. \tag{27}$$

For the solution we apply a heat transfer code described by Bühler (1993) to solve the problem iteratively using finite difference techniques. A more efficient way, however, would be to use a fast Poisson solver to invert the Laplaceans. Numerical calculations are performed on a finite domain which ends at $r = r_{\max} = 100$ ($\xi_{\max} = 4.6$). A grid with $n_\xi \times n_\varphi = 100 \times 500$ grid points was used for the calculations for a Hartmann number $Ha = 20$ based on the radius of the vapor channel. Calculations with other maximum radii did not show significant differences. The Hartmann layer which appears near $r = 1$ is resolved with a few grid points. For MHD duct flow such a low resolution would not be not sufficient since in that case the currents close through the layers so that the layers determine the whole solution. Here, the currents close though the core in a direction perpendicular to the computational domain. The physics is mainly governed by the flow outside the Hartmann layers. The role of the layer is to match the core vorticity $\omega = \nabla^2\psi$ with the condition at the interface where we have $\omega = 0$. The boundary layer for ω is therefore more expressed than the layer for ψ because the wall normal component of velocity does not change at the leading order across the layer as $Ha \gg 1$.

We show in Fig. 3 results for a Hartmann number $Ha = 20$ based on the radius of the vapor channel. We do not show results for smaller values but describe the phenomena briefly. In the hydrodynamic case when $Ha = 0$, the flow is purely radial. With

increasing Hartmann number the streamlines are shifted to a narrow region close to the y-axis where they are mainly parallel and aligned with the magnetic field. Details of the flow near the interface can be seen from Fig. 4. We see that the vorticity ω develops pronounced Hartmann layers in contrast to the streamfunction ψ. Both figures Figs. 4 and 3 show a minor fraction of the whole computational domain which extends to a radius of $r_{\max} = 100$. An overview of the flow in the whole domain is shown in the logarithmic plot in Fig. 5. The streamlines become straight with a slope of 2 in the far field and confirm so far the self-similar character of the solution in some distance from the vapor channel.

The interaction with the magnetic field favors the flow to use a direction parallel to the field in order to minimize Lorentz forces. Lorentz forces vanish if the flow is exactly aligned with the field. The above reasoning shows that there are no Lorentz forces along the y axis and along the z axis in some distance from the interface. Therefore there is no MHD pressure drop along y and along z because the fluid has the possibility to flow towards the interface aligned with the field. This result is a direct consequence of the assumption that the liquid domain has a large extension. In the next section we consider a case where the liquid domain has a finite extension along y. Such a restriction will force the flow to have a component of velocity perpendicular to the magnetic field, associated with an MHD pressure drop.

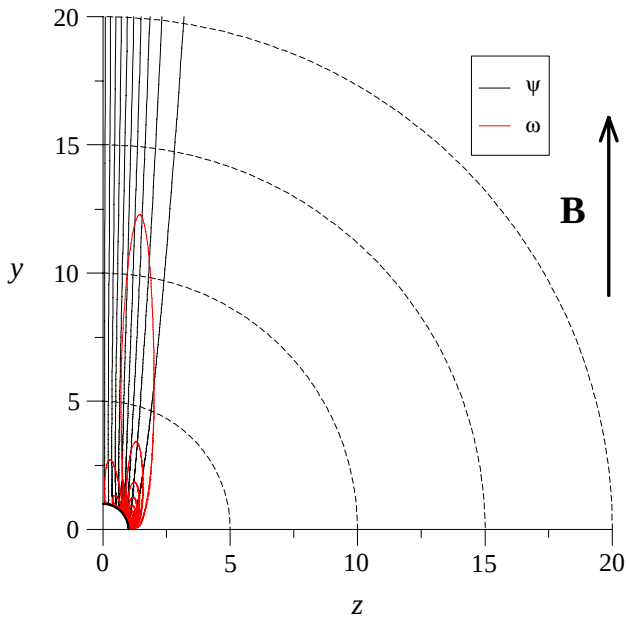

Figure 3: Streamlines (black) and isolines of vorticity (red) for a flow towards a circular vapor channel. $Ha = 20$, $r_{\max} = 400$

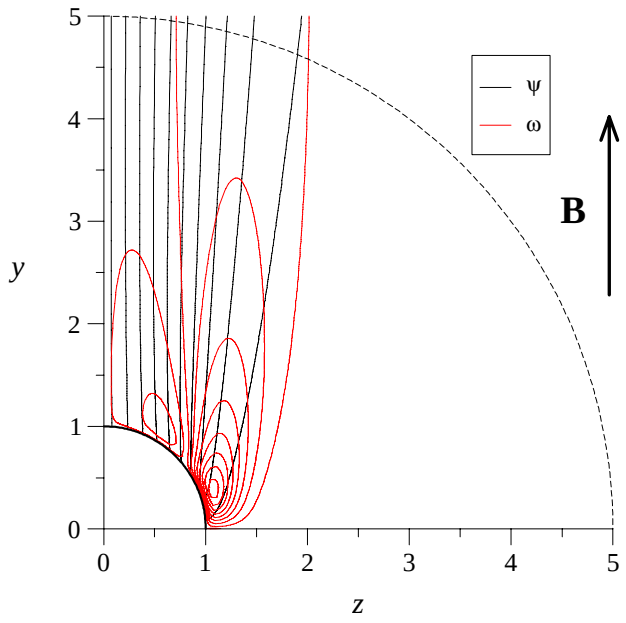

Figure 4: Streamlines (black) and isolines of vorticity (red) for a flow towards a circular vapor channel. Zoom of Fig. 3

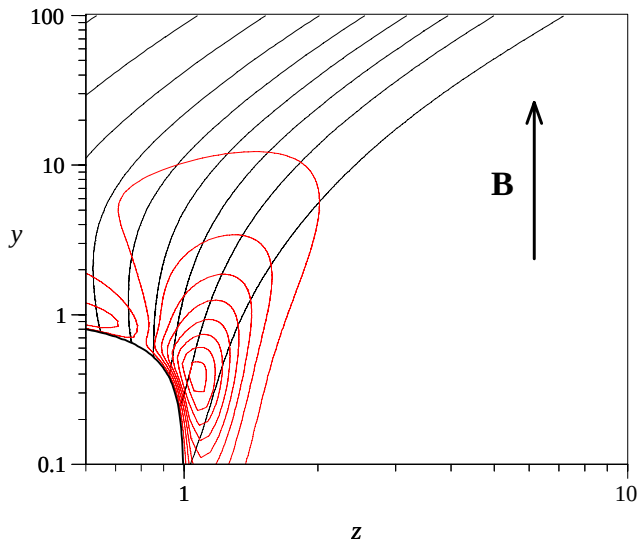

Figure 5: Streamlines (black) and isolines of vorticity (red) for a flow towards a circular vapor channel. $Ha = 20$, $r_{\max} = 400$ plotted for logarithmic axes.

4 Asymptotic analysis

In this section we consider the case when the vapor channels have a periodic appearance along y with nondimensional distance 2 measured along filed lines and spacing a in the transverse direction. In the following we use the half spacing along field lines as a characteristic length scale of the problem and assume that the magnetic field is large enough that the Hartmann layers are thin compared with the radius of the vapor channel. For details of the geometry see Figs. 1 and 6. The fluid is supplied to the volume considered at the nondimensional positions $z = \pm a$. We are mainly interested in the flow near the vapor-liquid interface and do not concern the question how the flow is carried towards the lateral borders. One could imagine that the fluid is supplied e.g. along magnetic field lines for $|z| > a$ with low MHD pressure drop.

For large Hartmann numbers the flow region splits into distinct subregions. These are for the present case the cores I and II and the viscous Hartmann and parallel layers with typical thickness of $\delta_h \sim Ha^{-1}$ and $\delta_p \sim Ha^{-1/2}$, respectively. We construct a composite solution for the unknowns such as

$$\omega = \omega_c + \omega_h + \omega_p, \tag{28}$$

$$\psi = \psi_c + \psi_h + \psi_p, \tag{29}$$

where the subscripts denote the contributions due to the solution in the inviscid cores and in the viscous Hartmann and parallel layers. The scales of the viscous layers become obvious if we eliminate the vorticity in (9) by the streamfunction according to (10) which yields

$$-\nabla^4\psi + Ha^2\partial_{yy}\psi = 0. \tag{30}$$

In order to describe the flow in the Hartmann layer we zoom into the layer by using the stretched coordinate $\eta = y/\delta_h$ with $\delta_h \ll 1$. This results in

$$-\frac{1}{\delta_h^4}\partial_\eta^4\psi + Ha^2\frac{1}{\delta_h^2}\partial_{\eta\eta}\psi = 0, \tag{31}$$

and an adequate balance of forces in the Hartmann layer determines the typical thickness of the layer as $\delta_h = Ha^{-1}$.

If we stretch the parallel layer by using the coordinate $\zeta = z/\delta_p$ the equation (30) becomes at leading order

$$-\frac{1}{\delta_p^4}\partial_\zeta^4\psi + Ha^2\partial_{yy}\psi = 0 \tag{32}$$

so that a balance of forces requires $\delta_p = Ha^{-1/2}$.

4.1 The Hartmann layers

We have already qualitatively seen that the role of the Hartmann layers is almost passive since the wall normal component of velocity does not change at leading order of approximation and we will support this observation now by arguments. We introduce

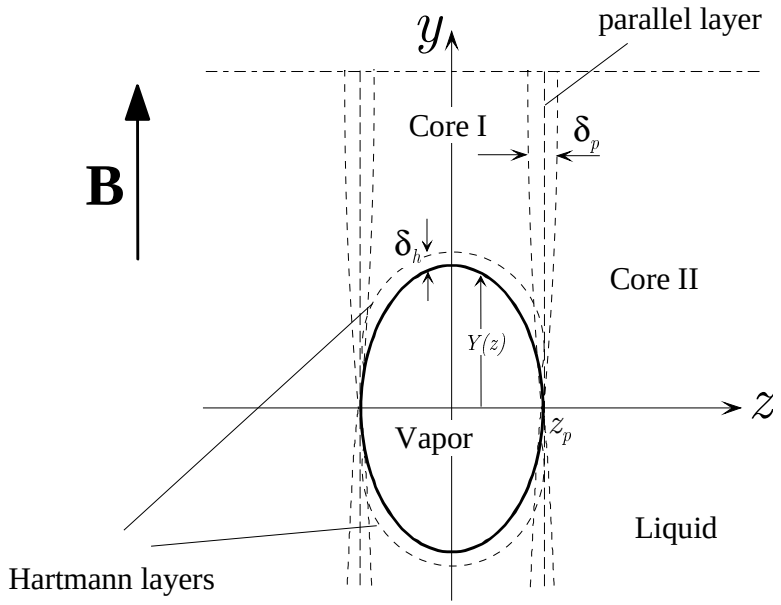

Figure 6: Two-dimensional model geometry with subregions

a stretched Hartmann layer coordinate $\eta = Ha\ (y - Y)$, where $Y(z)$ describes the contour of the vapor channel. It is assumed that the viscous contributions of the variables in the Hartmann layer depend mainly on this coordinate. Then (10) simplifies to

$$Ha^2 \partial_{\eta\eta}\psi_h + \omega_h = 0, \tag{33}$$

and when substituted in the vorticity equation (9) we find in the limit as $Ha \to \infty$

$$\partial_{\eta\eta}\omega_h - \omega_h = 0. \tag{34}$$

Here, ψ_h and ω_h denote the viscous corrections in the Hartmann layers to the inviscid core solution. The solution for vorticity inside the layer is purely exponential,

$$\omega_h = -\omega_c \exp(-\eta). \tag{35}$$

It matches the core solution $\omega_h \to 0$ as $\eta \to \infty$ with the interface condition $\omega_h = -\omega_c$ at $\eta = 0$. The streamfunction ψ_h does not change across the Hartmann layer at leading order of approximation. This can be shown by integration of (33) between η and ∞. With the requirement that the viscous corrections vanish as $\eta \to \infty$ we find

$$\psi_h = Ha^{-2}\omega_c \exp(-\eta). \tag{36}$$

We have therefore no viscous correction of the streamfunction across the Hartmann layer at leading order so that we can apply the condition (13) at the interface directly to the core solution

$$\partial_t \psi_c = -1 \quad \text{at } y = Y. \tag{37}$$

4.2 The core

In the core the equations (9) and (10) reduce for $Ha \to \infty$ to

$$\partial_{yy}\psi_c = 0, \tag{38}$$
$$\omega_c = -\nabla^2\psi_c. \tag{39}$$

It is possible to determine ψ_c by integration of (38) with the result

$$\psi_c = \psi_\Gamma \frac{1-y}{1-Y}, \tag{40}$$

where the value of the streamfunction on the interface ψ_Γ and the contour function Y depend on the transverse coordinate z. The pressure gradient in the core is obtained with Ohm's law (8) as $\partial_z p = j = \partial_y \psi_c$ which gives

$$\partial_z p = -\frac{1}{1-Y}\psi_\Gamma. \tag{41}$$

For small vapor channels, say $Y \ll 1$, we can estimate the pressure drop required to drive the flow from $z = a$ towards the interface. Then $\partial_z p \approx -\psi_\Gamma$ and the pressure drop becomes

$$\Delta p = -a\psi_{\max}, \tag{42}$$

where $\psi_{\max}$ stands for the total flow rate that enters the vapor channel from the quarter $0 < y < 1$, $0 < z < a$. For details of the geometry see Fig. 6.

If we return to dimensional quantities we have

$$\Delta p^* = -a\psi^*_{\max}\sigma B^2. \tag{43}$$

The superscript '*' has been introduced to denote dimensional values of pressure and flow rate. The dimensional flow rate $\psi^*_{\max}$ is determined by the volumetric heating q such that the latent heat during evaporation equals the heat input in the volume element

$$\rho H \psi^*_{\max} = -qaL^2. \tag{44}$$

The variable H stands for the heat of evaporation. This leads to a pressure drop

$$\Delta p^* = \frac{q\sigma\,(aL)^2\,B^2}{\rho H} = v_0\,\sigma a L B^2, \tag{45}$$

with a typical velocity

$$v_0 = \frac{q\,aL}{\rho H}. \tag{46}$$

In two-phase flow literature a characteristic velocity is the superficial vapor velocity v_g (Whalley (1987)), which differs from our v_0 by the density ratio between the liquid and the vapor phase.

Finally we can compare the pressure drop with the hydrostatic pressure head which is required to drive the flow $\rho g\, \Delta x^* = \Delta p^*$ and find

$$\frac{\Delta x^*}{aL} = \frac{v_0\, \sigma B^2}{\rho g} = FrN, \tag{47}$$

where N is the interaction parameter based on v_0 and

$$Fr = \frac{v_0^2}{aLg} \tag{48}$$

is a Froude number. Now we introduce the physical data of the EVOLVE concept.

$$\begin{array}{llll} \rho = & 414 & \frac{\mathrm{kg}}{\mathrm{m}^3} & \\ \sigma = & 1.8 \cdot 10^6 & \frac{\mathrm{A}}{\mathrm{Vm}} & q = \quad 20 \cdot 10^6 \quad \frac{\mathrm{W}}{\mathrm{m}^3} \\ H = & 2.0 \cdot 10^7 & \frac{\mathrm{J}}{\mathrm{kg}} & \\ T = & 0.237 & \frac{\mathrm{N}}{\mathrm{m}} & B = \quad 10 \qquad \mathrm{T} \end{array} \tag{49}$$

A tray evaporation scenario makes sense only if the liquid surface is sufficiently flat. This requires that the surface slope is small,

$$\frac{\Delta x^*}{aL} = \frac{v_0\, \sigma B^2}{\rho g} < 1, \tag{50}$$

a condition that determines the characteristic velocity as

$$v_0 < \frac{\rho g}{\sigma B^2} = 2.3 \cdot 10^{-5} \frac{\mathrm{m}}{\mathrm{s}}. \tag{51}$$

It should be mentioned here that v_0 is the uniform velocity in the core II. The normal component of velocity at the interface differs from this by a factor given by the ratio of the regular spacing along y and the arc length of the interface in the considered sector. The reason is that the flow rate carried by the uniform core velocity must cross the much shorter interface. The characteristic velocity is related by (46) with the geometrical scales. This condition determines the maximum spacing of vapor channels in a direction perpendicular to the field as

$$aL = \frac{\rho H v_0}{q} < 0.95\,\mathrm{cm}. \tag{52}$$

Finally we determine the pressure drop required to drive the flow towards the vapor channels and find

$$\Delta p^* < 39\ \mathrm{Pa}, \tag{53}$$

a value that seems to be really small.

4.3 The interface

It has been shown in a number of references that the pressure is uniform along magnetic field lines and does not vary across the Hartmann layer at the leading order of approximation (see e.g. Moreau (1990)). This means that the pressure calculated form

(41) can be taken as the liquid pressure at the interface. We assumed above that the vapor conditions are uniform in the cross section of the vapor channel so that the vapor pressure p_v at the interface is constant in the cross section considered. This leads to a pressure difference between the vapor and the liquid that varies along the interface. This difference in pressure can be balanced only by a varying curvature in the condition for the pressure jump across an interface (Milne-Thomson (1974))

$$p_v - p = T\,K, \tag{54}$$

where, in the present notation, T stands for the surface tension scaled by $\sigma v_0 B^2 L^2$ and K is the nondimensional curvature. It can be expressed in terms of the contour function Y or its derivatives $\partial_z Y = Y'$ as

$$K = \frac{Y''}{\left(1 + Y'^2\right)^{3/2}}. \tag{55}$$

We take the derivative of (54) with respect to z and find a relation that can be combined with (41) to give

$$\psi_\Gamma = T\,(1 - Y)\;\partial_z K. \tag{56}$$

For efficient calculations one can describe the contour in cylindrical coordinates by its distance from the origin $R(\varphi)$ and express the curvature as

$$K = \frac{R^2 + 2R'^2 - RR''}{\left(R^2 + R'^2\right)^{3/2}}. \tag{57}$$

The contour function becomes $Y = R\cos\varphi$ and the transverse derivative at the interface can be expressed as

$$\partial_z = \frac{1}{R\cos\varphi}\partial_\varphi. \tag{58}$$

We know further that ψ_Γ is proportional to the arc length measured along the contour

$$\psi_\Gamma = -\int \sqrt{R^2 + R'^2}\,d\varphi. \tag{59}$$

Substituted into (56) yields after differentiation with respect to φ

$$-\sqrt{R^2 + R'^2} = T\,\partial_\varphi\left(\frac{1 - R\cos\varphi}{R\cos\varphi}\partial_\varphi K\right). \tag{60}$$

This equation is solved with boundary conditions

$$R(0) = R_0, \quad R'(0) = 0, \quad R'''(0) = 0, \quad R'(\pi/2) = 0. \tag{61}$$

The value of R_0 determines the size of the vapor channel measured along magnetic field lines. The conditions that $R'(0) = R'(\pi/2) = 0$ result from symmetry with respect to the y and z axis. The symmetry of the pressure field with respect to the y axis requires $R'''(0) = 0$. For strong magnetic fields the channels will become highly elongated. Then,

$R'(\pi/2) = 0$ looses its physical relevance. The solution of (60) is meaningful only up to the position φ_1, where the contour has a vertical tangent given by

$$R' \sin \varphi_1 + R \cos \varphi_1 = 0. \tag{62}$$

The solution for the contour has then to be completed by a vertical straight line. Since the curvature of this line is zero, there is no jump in pressure across the interface along the line. Therefore, at the point where the straight line meets the solution of (60) a jump in pressure has to be excluded. This requires that the curvature calculated from $R(\varphi)$ vanishes also at $\varphi = \varphi_1$,

$$R^2 + 2R'^2 - RR'' = 0 \quad \text{at } \varphi = \varphi_1. \tag{63}$$

The solution of (60) is obtained numerically by using MAPLE routines with initial conditions

$$R(0) = R_0, \;\; R'(0) = 0, \;\; R''(0) = \alpha, \;\; R'''(0) = 0. \tag{64}$$

The shooting parameter α is chosen such that either all conditions in (61) are satisfied or if a vertical tangent appears at $\varphi_1 < \pi/2$ we chose α such that (63) is satisfied, i.e. that the curvature vanishes at φ_1.

The resulting contours of the vapor channels are displayed in Fig. 7. If the surface tension dominates magnetic forces, when $T/Y(0)^3 \gg 1$ the shape of vapor channels is circular. The vapor cross sections start to become elongated along field lines if both forces become comparable. For $T/Y(0)^3 \ll 1$ the elongation is dominant and contours become possible where a major part of the interface is straight and aligned with the field. The maximum width of such channels seems to be proportional to $T^{1/3}$ for small T.

If we use the physical data of EVOLVE and the velocity v_0 as estimated above the surface tension parameter becomes $T = 1$ and $T = 0.01$ for a spacing of the vapor channels in the direction of the magnetic field $L = 0.01\,\mathrm{m}$ and $L = 0.1\,\mathrm{m}$, respectively. This means that the elongation of the cross sections along magnetic field lines is moderate or small.

4.4 Flow pattern

During the previous subsection we determined the shape of the interface, $R(\varphi)$. These results determine the streamfunction along the vapor-liquid interface according to (59) and yield with (40) the flow field outside the viscous layers. Results are displayed in Figs. 8, 9 and 10 which show streamlines towards vapor channels. The extension of the channels along field lines is $Y(z = 0) = 0.3$ and the surface tension parameters are $T = 0.1,\ 0.01$ and 0.001, respectively. Cases with larger values of T do not differ qualitatively from results shown here for $T = 0.1$. In all cases internal parallel layers develop along the magnetic field line which is tangential to the contour of the vapor channel at $z = z_p$. To the right of the parallel layer for $z > z_p$ the flow is parallel and oriented perpendicular to the magnetic field. The velocity is uniform along field lines since the isolines of the streamfunction are equidistant. To the left of the internal layer for $0 < z < z_p$ the streamlines have a shape similar to hyperbolas centered at $y = 1$,

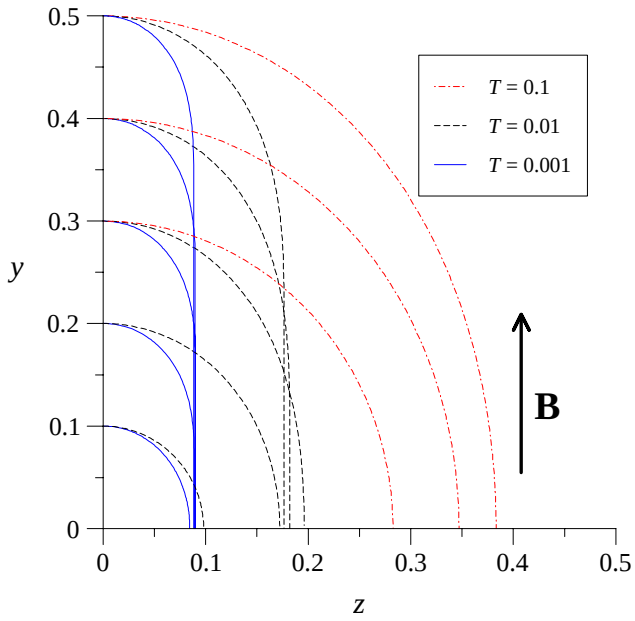

Figure 7: Shapes of vapor channels for different values of surface tension and channel size.

$z = 0$. For $T = 0.1$ and 0.01 the solutions to the right and to the left are continuous across the internal layer but exhibit discontinuous slopes at $z = z_p$. Here the role of the internal layer is more or less passive since it smooths *only* the discontinuous y component of velocity. For $T = 0.001$ the situation is different. Here we have a contour which is aligned with the field not only in one point but along a large portion of the contour surface. All liquid which crosses the parallel portion of the interface is carried by the parallel layer along field lines. An $O(1)$ flow rate carried within a layer of thickness $\delta_p \sim Ha^{-1/2}$ requires a high-velocity jet with velocities on the order $v \sim Ha^{1/2}$. This leads to the fact observed in Fig. 10 that now the streamfunction becomes discontinuous across the parallel layer. Parallel layers similar to the present one occur in buoyant magneto-convection in horizontal Bridgman crystal growth as reported by Garandet, Albousière and Moreau (1992). These authors find, as we do in the present case, a flow with parallel streamlines oriented perpendicular to the magnetic field in some distance from the parallel layer. Within a layer of thickness $\delta_p \sim Ha^{-1/2}$ the flow is redistributed in a high-velocity jet near a wall aligned with the magnetic field. If details about the flow in the internal parallel layer are required it should be possible to reconstruct such a flow from the solutions in both cores.

In order to confirm the results obtained by the asymptotic analysis we compare streamlines with those obtained by a numerical solution at a large Hartmann number. The most simple comparison is possible for a case where the shape of the interface is nearly circular. This allows us to use the same numerical procedure as outlined above for which we used the polar coordinate system. The only difference is that the inflow conditions are different. Instead of (27) we have now a uniform inflow perpendicular to

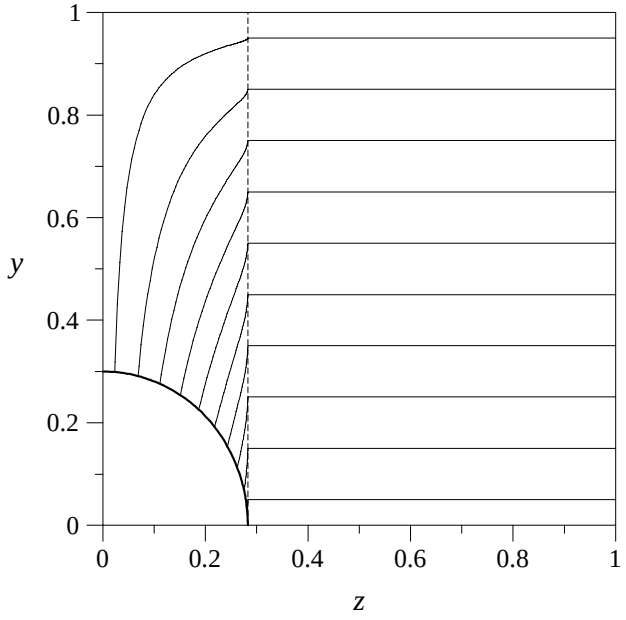

Figure 8: Streamlines for $T = 0.1$ and $Y(0) = 0.3$

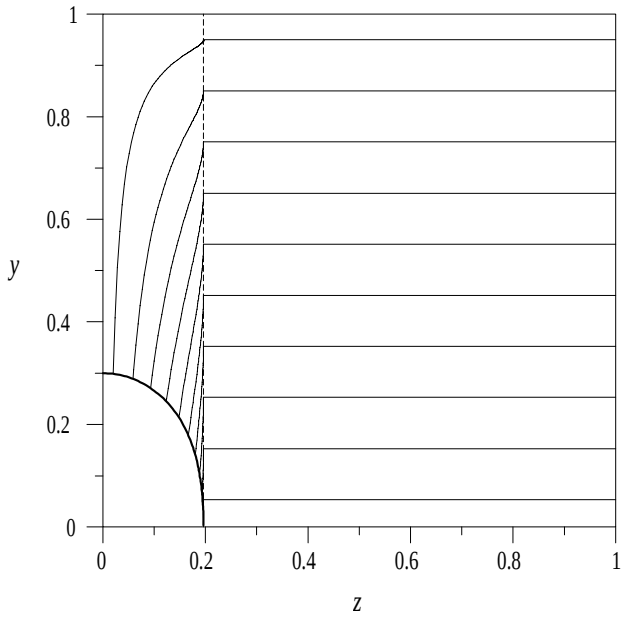

Figure 9: Streamlines for $T = 0.01$ and $Y(0) = 0.3$

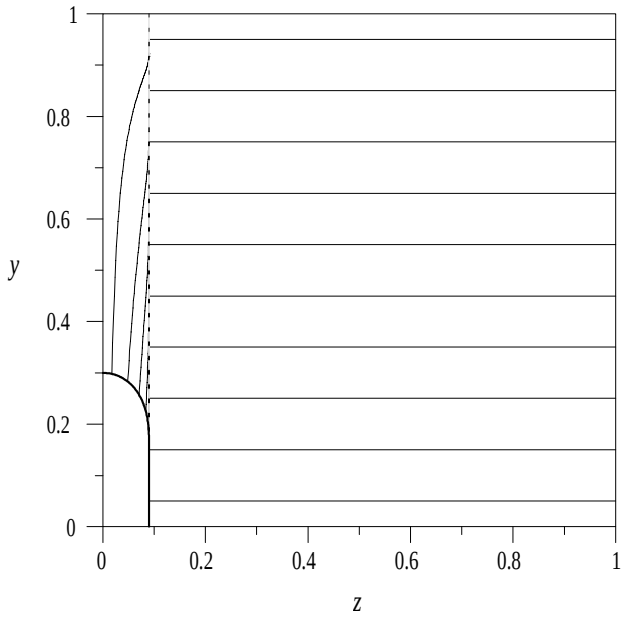

Figure 10: Streamlines for $T = 0.001$ and $Y(0) = 0.3$

the applied magnetic field. In terms of the streamfunction the inflow condition becomes

$$\psi = \cos\varphi - 1, \;\; \omega = 0 \quad \text{at } r = 1, \tag{65}$$

while the condition at the interface

$$\psi = -\frac{2}{\pi}\varphi\,, \;\; \omega = 0 \quad \text{at } r_\Gamma, \tag{66}$$

is posed now at a radius $r_\Gamma < 1$ due to a different scaling of the problem. In the present problem the Hartmann number is $Ha = 500$. A comparison shows a good agreement of both solutions in some distance from the internal parallel layer of thickness $\delta_p \sim O\left(Ha^{-1/2}\right)$. The comparison of streamlines is shown in Fig. 11.

4.5 Three-dimensional considerations

We assumed above that the 2D flow in horizontal planes is driven by the hydrostatic pressure head of the liquid pool. This required considerable surface slopes to overcome the MHD pressure drop when driving the flow towards the vapor channels. The present analysis is based on the assumption that the flow is two-dimensional in horizontal planes perpendicular to the vapor channels. This assumption seems to be justified in most of the liquid domain, i.e. in the cores. We have seen that the currents are perpendicular to this plane, parallel to the vapor channels. At the bottom of the tray the currents may enter or leave the electrically conducting solid wall and close their path within the wall. If the wall is highly conducting the influence from the bottom on the 2D flow will be small. The situation is schematically shown in Fig. 12 which displays a vertical plane through a vapor channel. On the free surface of the liquid pool, however, the situation

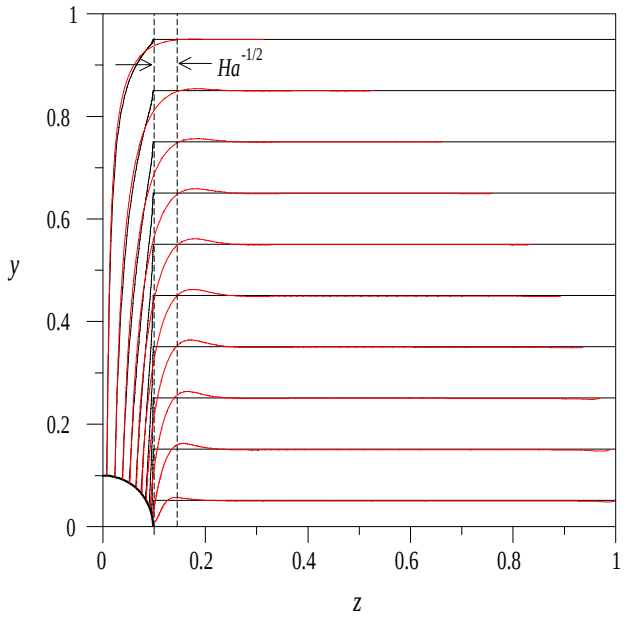

Figure 11: Streamlines calculated from a numerical solution (red) compared with those obtained by the asymptotic analysis (black) for $Ha = 500$, $Y(0) = 0.1$ and $T = 0.01$.

is different. A closure of currents must establish within the fluid with the consequence that the flow looses its 2D nature. While in the core the Lorentz forces $\mathbf{f}$ oppose the fluid motion, the Lorentz forces near the top have a direction perpendicular to the free surface. The Lorentz forces near the free surface decrease the pressure from the surface where we have $p = p_\infty$ to approach the core value p_c. We will show below that the pressure difference $\Delta p_t = p_\infty - p_c$, which gives an additional forcing to drive the flow towards the vapor channel, balances at least partly the MHD pressure drop. We regain by this mechanism the energy which has been lost by MHD braking in the core. The core extracts mechanical energy from the system and transfers it into electrical energy. This is carried by the currents to the top surface where it is released in order to keep the surface elevation rather constant instead of highly inclined towards the channels. We have seen above that variations of variables along field lines do not occur and that currents j_y are absent in the core. A balance of charge in a volume element reads

$$\partial_x j_x = -\partial_z j_z. \tag{67}$$

This relation may be integrated along x from the core to the surface where $j_x = 0$.

$$j_c = \int \partial_z j_z dx. \tag{68}$$

If we recall that according to (1) $j_z \approx -\partial_x p$ for small viscous forces we find

$$j_c = -\partial_z \int \partial_x p dx = -\partial_z \Delta p_t, \tag{69}$$

and when j_c is substituted by the gradient of core pressure we arrive at

$$\partial_z \left(p_c + \Delta p_t \right) = 0 \tag{70}$$

or at

$$p_c + \Delta p_t = constant = p_\infty. \tag{71}$$

This result confirms that a surface slope is not required to overcome the MHD pressure drop at first approximation. Therefore we could relax the condition for a maximum allowable core velocity and permit even larger spacings between the vapor channels as were estimated in Sect. 4.2. Nevertheless, we must keep in mind that the outlined situation is idealized and that some currents may escape from the charge balance in the top layer also along the y-direction. These currents do not contribute to Δp_t so that we can not recover the whole MHD pressure drop.

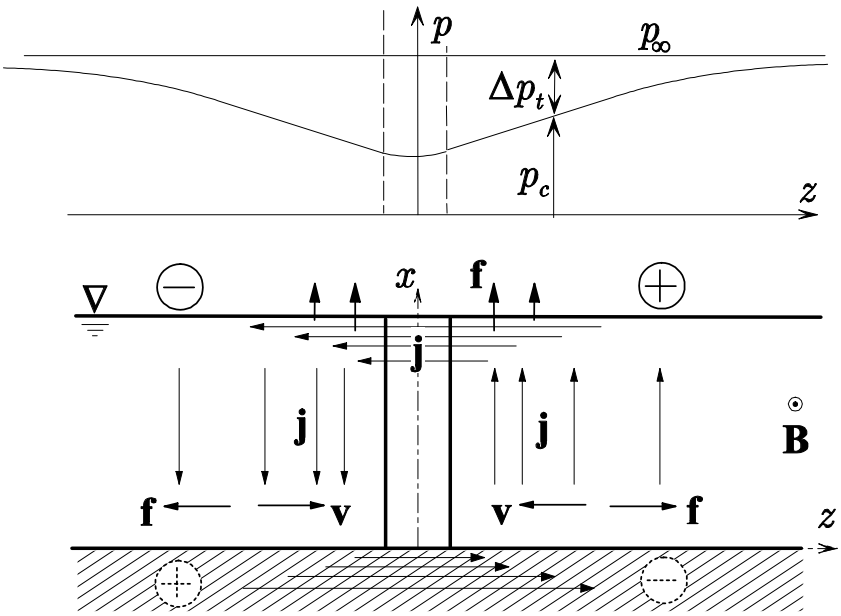

Figure 12: Sketch of current paths, Lorentz forces and pressure distribution.

There is another point that should be stressed in the present discussion. The currents which flow in the horizontal direction require a driving potential gradient, both near the top and at the bottom as indicated by the symbols $\oplus$ and $\ominus$ in Fig. 12. This leads to a formation of a vertical potential gradient $\partial_x \phi$ as well, which, at large distance from the vapor channel, balances the induced electric field. As a consequence the currents, the Lorentz forces, and the MHD pressure drop vanish when $\partial_x \phi \to -w$ as $|z| \to \infty$. Nevertheless, everything shown above should be correct in some vicinity of the vapor channel as long as the transverse distance $|z|$ is small compared with the height of the liquid layer. For larger transverse distances from the vapor channel the flow approaches solutions known for MHD free-surface flows as described e.g. by Molokov and Reed (1999). More accurate results for the resent problem require a detailed 3D analysis which is out of the scope of the present work.

5 Conclusions

The magnetohydrodynamic flow in the liquid lithium phase during a specific boiling scenario proposed for the EVOLVE concept of a fusion blanket has been investigated. In the EVOLVE concept one possible boiling scenario is based on the formation of permanent vapor channels at the surface of which the heat is removed by evaporation. The prove that such a boiling scenario is possible was not the subject of the present work. Numerical and asymptotic analyses showed that near the vapor channels the flow is mainly parallel to the applied magnetic field. Depending on the inflow conditions the parallel layers that spread along the field lines which are tangential to the vapor channel become more or less important. Especially for the case when the channels have a periodic occurrence along field lines the liquid has to be supplied from a direction perpendicular to the magnetic field. Then, at large distance from the vapor channel the flow has a uniform velocity with equidistant streamlines. When the liquid approaches the parallel layer the flow turns and follows streamlines with hyperbola like shape before it reaches the liquid-vapor interface. Depending on the surface tension parameter and the size of the vapor channel the interface may be elongated along field lines or remain circular. For EVOLVE we expect only moderate or small elongations. The evaluation of the pressure drop for typical data of the EVOLVE concept gives acceptably small values.

References

Anderson, M. H., Murphy, J. G., Sawan, M. E., Sviatoslavsky, I. N., Corradini, M. L. and Malang, S.: 2000, EVOLVE lithium tray thermal-hydraulic analysis, *ANS 14th Topical Meeting on the Technology of Fusion Energy, Parc City, Utah, USA, October 15-19*.

Bühler, L.: 1993, Convective-diffusive transport in laminar MHD flows, *Technical Report KfK 5241*, Kernforschungszentrum Karlsruhe.

Garandet, J., Albousière, T. and Moreau, R.: 1992, Buoyancy driven convection in a rectangular enclosure with a transverse magnetic field., *Int. J. Heat Mass Transfer* **35**(4), 741–748.

Milne-Thomson, L. M.: 1974, *Theoretical Hydrodynamics*, fifth edn, MACMILLAN PRESS LTD, London, Basinstoke.

Molokov, S. and Reed, C. B.: 1999, Review of free-surface MHD experiments and modelling, *Technical Report ANF/TD/TM99-08*, Argonne National Laboratory.

Moreau, R.: 1990, *Magnetohydrodynamics*, Kluwer Academic Publisher.

Whalley, P. B.: 1987, *Boling, Condensation and Gas-Liquid Flows*, Clarendon Press, Oxford.